

---

# Schur's Positive-Definite Network: Deep Learning in the SPD cone with structure

---

**Can Pouliquen**  
can.pouliquen@ens-lyon.fr

**Mathurin Massias**  
mathurin.massias@inria.fr

**Titouan Vayer**  
titouan.vayer@inria.fr

Univ Lyon, ENS Lyon, UCBL, CNRS, Inria, LIP, F-69342, LYON Cedex 07, France.

## Abstract

Estimating matrices in the symmetric positive-definite (SPD) cone is of interest for many applications ranging from computer vision to graph learning. While there exist various convex optimization-based estimators, they remain limited in expressivity due to their model-based approach. The success of deep learning has thus led many to use neural networks to learn to estimate SPD matrices in a data-driven fashion. For learning structured outputs, one promising strategy involves architectures designed by unrolling iterative algorithms, which potentially benefit from inductive bias properties. However, designing correct unrolled architectures for SPD learning is difficult: they either do not guarantee that their output has all the desired properties, rely on heavy computations, or are overly restrained to specific matrices which hinders their expressivity. In this paper, we propose a novel and generic learning module with guaranteed SPD outputs called SpodNet, that also enables learning a larger class of functions than existing approaches. Notably, it solves the challenging task of learning jointly SPD and sparse matrices. Our experiments demonstrate the versatility of SpodNet layers.

## 1 Introduction

The estimation of symmetric positive-definite (SPD) matrices is a major area of research, due to their crucial role in various fields ranging such as optimal transport (Bonet et al., 2023; Ju and Guan, 2022; Yair et al., 2019), graph theory (Lauritzen, 1996), computer vision (Nguyen et al., 2019) or finance (Ledoit and Wolf, 2003). While various statistical estimators, i.e. *model-based*, have been developed (Ledoit and Wolf, 2004; Banerjee et al., 2008; Cai et al., 2011), a more recent trend is to use *learning-based* approaches to estimate SPD matrices with neural networks (Gao et al., 2020).

Training neural networks while enforcing non-trivial structural constraints such as positive-definiteness is a difficult task. There have been many efforts in this direction in recent years, often in an ad-hoc manner and each with their own shortcomings (see Section 2 for more details). Building on the seminal work of Gregor and LeCun (2010) in sparse coding, a promising research direction involves designing neural networks architectures from the unrolling of an optimization algorithm (Chen and Pock, 2016; Monga et al., 2021; Chen et al., 2022). In the case of SPD matrices, algorithm unrolling presents several challenges. First, algorithms operating in the SPD cone usually rely on heavy operations such as retractions (Boumal, 2023), SVD or line search (Rolfs et al., 2012). These operations do not integrate well into a neural network architecture, making these algorithms difficult to unroll.

Second, beyond ensuring positive definiteness, it is often desirable to impose additional structure on the matrix to estimate, such as elementwise sparsity. Simultaneously enforcing SPD + sparsity constraints on the output of a neural architecture is extremely difficult (Guillot and Rajaratnam, 2015; Sivalingam, 2015). So far, it is only a hypothetical property that is not satisfied in practice (see Figure 2 and Section 5 for more details).

**Contributions:** In this paper, we combine the strengths of both model-based and data-driven approaches and we make the following contributions:

- We introduce a novel framework for building learning modules with a guaranteed SPD-to-SPD mapping for which it is also possible to enforce additional constraints on the output. We refer to it as SpodNet for *Schur’s Positive-Definite Network*. Our approach is originally inspired by the block-matrix updates perspective of the Graphical Lasso solver (Mazumder and Hastie, 2012) and extended to generic SPD learning. As a particular case, SpodNet layers are able to learn jointly SPD and sparse matrices in a data-driven fashion. To the best of our knowledge, SpodNet-based architectures are the first to offer strict guarantees combining both properties.
- We illustrate the framework’s versatility through applications in sparse precision matrix estimation. In this scenario, we present limitations of other learning-based approaches and demonstrate how to overcome them with SpodNet layers. Our experiments validate the use of SpodNet for learning jointly SPD-to-SPD and sparsity inducing functions, and show promising results across various performance metrics.

**Notation** We reserve the bold uppercase for matrices  $\Theta$ , bold lowercase  $\theta$  for vectors and standard lowercase  $\theta$  for scalars. The soft-thresholding function is  $\text{ST}_\gamma(\cdot) = \text{sign}(\cdot) \max(|\cdot| - \gamma, 0)$  for  $\gamma \geq 0$ ; it acts elementwise on vectors or matrices. On matrices,  $\|\cdot\|_1$  is the sum of absolute values of the matrix coefficients. The cone of SPD matrices in dimension  $p$  is denoted  $\mathbb{S}_{++}^p$ . We use  $\Sigma$  to designate covariance matrices,  $\Theta$  for precision matrices, and  $S$  for empirical covariance matrices.

## 2 Related works

Before delving into the details of SpodNet, we briefly review existing approaches for constructing SPD matrices, which can be broadly divided into three categories.

**Riemannian learning** Riemannian optimization provides tools to build algorithms whose iterates lie on Riemannian manifolds, such as the SPD manifold (Absil et al., 2008). Many have adopted these tools to design neural architectures that operate on the manifold of SPD matrices (Huang and Van Gool, 2017; Gao et al., 2020, 2022). However, a common and major bottleneck of these models is their dependence on Riemannian operations which are notoriously costly to compute. Furthermore, Riemannian optimization beyond smooth objective functions is still an active area of research (Absil and Hosseini, 2019; Huang and Wei, 2022; Zhou et al., 2023) and it is thus highly non-trivial to design neural architectures to handle additional constraints such as *elementwise* sparsity.

**Projection-based methods** For some applications, it is of interest to project the matrices from a high-dimensional SPD manifold to a lower-dimensional one (Dong et al., 2017; Nguyen et al., 2019). Using linear algebra principles, these approaches design specific layers to guarantee that the final matrix is SPD. However, these solutions are ad-hoc and lack straightforward extensions for general SPD-to-SPD learning with additional structural constraints. Specifically, there is no obvious way to incorporate elementwise sparsity on the matrices without risking breaking their SPD structure. For instance, hard-thresholding the off-diagonal entries of a SPD matrix does not always preserve the SPD property (Guillot and Rajaratnam, 2012) and, more generally, elementwise functions preserving this property are very limited (Guillot and Rajaratnam, 2015).

**Unrolled learning** In order to ensure that a network’s output strictly respects some desired properties, another recent and successful direction is to unroll convex optimization algorithms (Chen et al., 2022). This unrolling procedure acts as an “inductive bias” on the architecture (Shrivastava, 2020), naturally guiding the model to explore suitable solutions within the space of imposed properties. In SPD learning, this approach has been exploited by Shrivastava et al. (2019) who unrolled an optimization algorithm to train neural networks to estimate sparse inverses of covariance matrices.

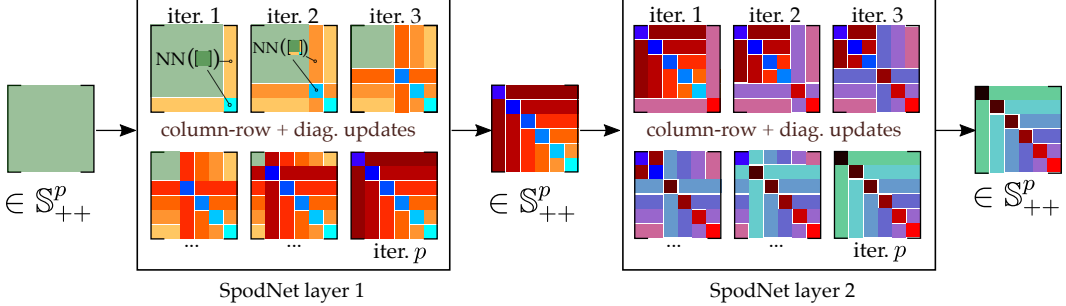


Figure 1: Schematic overview of SpodNet layers. Our framework chains updates of column-row pairs and diagonals using neural networks (note: the updated columns and rows are not constant, despite being represented by constant colors). At all times the matrices remain SPD via Schur’s condition.

Whilst algorithm unrolling is a very powerful approach to learn specific matrices, it is very difficult to extend it to generic SPD learning. We provide more details about the limits of related work in this setting in [Section 4.2](#).

### 3 The SpodNet framework

We now introduce the SpodNet layer which is at the core of our contribution. Essentially, it is an SPD-to-SPD mapping parameterized by neural networks. As described in [Section 4](#), SpodNet is inspired by an algorithm used to solve the Graphical Lasso in [Mazumder and Hastie \(2012\)](#). A SpodNet layer operates by cycling through the  $p$  column-row pairs individually and *i*) updating the corresponding column-row with a neural network, and *ii*) updating the diagonal element to maintain the SPD constraint (see [Figure 1](#)). Interestingly, the neural network at step *i*) can update the column-row to *any* value without compromising the SPD guarantee. Consequently, one is free to exploit a spectrum of approaches for those updates depending on other desired structural properties of the output matrix. In particular, we describe in [Section 4](#) a specific implementation of SpodNet that enforces elementwise sparsity for learning sparse precision matrices.

#### 3.1 Algorithmic foundations

More formally, when the SpodNet layer operates on the  $i$ -th column and row of  $\Theta \in \mathbb{S}_{++}^p$  it also updates the  $i$ -th diagonal coefficient accordingly. The key to preserving the positive-definiteness of the matrix upon changing its  $i$ -th column and row is an appropriate update of the diagonal entry  $\Theta_{ii}$  based on Schur’s condition for positive-definiteness. In the following, a  $+$  superscript on a variable (e.g.  $\theta^+$ ) indicates an update value of this variable (e.g. outputted by a neural network). The following proposition formalizes the SpodNet operations.

**Proposition 3.1.** *Suppose the updated column-row pair is the last one ( $i = p$ ). We partition  $\Theta$  as*

$$\Theta = \begin{bmatrix} \Theta_{11} & \theta_{12} \\ \theta_{21} & \theta_{22} \end{bmatrix}, \quad \text{with } \Theta_{11} \in \mathbb{R}^{(p-1) \times (p-1)}, \theta_{12} \in \mathbb{R}^{p-1}, \theta_{21} = \theta_{12}^\top, \theta_{22} \in \mathbb{R}. \quad (1)$$

(for a generic column  $i$ ,  $\Theta_{11}$  refers to  $\Theta$  without its  $i$ -th row and  $i$ -th column,  $\theta_{12}$  is the  $i$ -th row of  $\Theta$  without its  $i$ -th value, and  $\theta_{22}$  is  $\Theta_{ii}$  as illustrated in [Algorithm 1](#)).

Let  $f : \mathbb{R}^{p \times p} \rightarrow \mathbb{R}^{p-1}$ ,  $g : \mathbb{R}^{p \times p} \rightarrow \mathbb{R}_{++}$ , where  $f$  and  $g$  are arbitrary functions. Then, updating the  $i$ -th row and column of  $\Theta$  as

$$\Theta^+ \triangleq \begin{bmatrix} \Theta_{11} & \theta_{12}^+ \triangleq f(\Theta) \\ \theta_{21}^+ \triangleq f(\Theta)^\top & \theta_{22}^+ \triangleq g(\Theta) + \theta_{21}^+ [\Theta_{11}]^{-1} \theta_{12}^+ \end{bmatrix}, \quad (2)$$

preserves the SPD property, i.e.  $\Theta^+ \in \mathbb{S}_{++}^p$ .

*Proof.* Since  $\Theta$  is positive-definite, so is its leading principal submatrix  $\Theta_{11}$ . It follows that  $\Theta^+$  is well-defined, and obviously symmetric. Its positive-definiteness then ensues from Schur's condition for positive-definiteness. Indeed  $\Theta^+$  is SPD when  $\Theta_{11} \succ 0$  and  $\theta_{22}^+ - \theta_{12}^{+\top} [\Theta_{11}]^{-1} \theta_{12}^+ = g(\Theta) > 0$  (Zhang, 2006, Theorem 1.12). The latter condition is ensured as the output of  $g$  is a positive scalar.  $\square$

Finally, one SpodNet layer chains  $p$  updates of the form (2), sequentially updating all column-row pairs one after the other as summarized in Algorithm 1. A full SpodNet architecture then stacks  $K$  SpodNet layers. The overall procedure is schematized in Figure 1 for  $K = 2$ .

The expressivity of SpodNet comes from the simple realization that one is free to plug *any* arbitrary functions  $f$  and  $g$  in the updates whilst guaranteeing that  $\Theta$  remains in the SPD cone. Namely, additional structure such as sparsity can trivially be imposed on  $\Theta$  through  $f$ . We next detail the computational cost of fully updating  $\Theta$  through one SpodNet layer.

### 3.2 Improving update complexity

The update of Equation (2) a priori requires inverting the matrix  $\Theta_{11}$  which comes with a prohibitive cost of  $\mathcal{O}(p^3)$  for each column-row update. We can fortunately leverage the column-row structure of the updates to decrease the cost to a mere  $\mathcal{O}(p^2)$ , by maintaining the matrix  $\mathbf{W} = \Theta^{-1}$  up-to-date along the iterations.

**Proposition 3.2.** Let  $\mathbf{W}$  be the inverse of  $\Theta$ , adopting the same block structure  $\mathbf{W} = \begin{bmatrix} \mathbf{W}_{11} & \mathbf{w}_{12} \\ \mathbf{w}_{12}^\top & w_{22} \end{bmatrix}$ .

Then  $[\Theta_{11}]^{-1} = \mathbf{W}_{11} - \frac{1}{w_{22}} \mathbf{w}_{12} \mathbf{w}_{12}^\top$ . In addition, if  $\Theta$  is updated as  $\Theta^+$  following Equation (2), then the update of  $\mathbf{W}$  defined by

$$\mathbf{W}^+ \triangleq \begin{bmatrix} [\Theta_{11}]^{-1} + \frac{[\Theta_{11}]^{-1} \theta_{12}^+ \theta_{21}^+ [\Theta_{11}]^{-1}}{g(\Theta)} & -\frac{[\Theta_{11}]^{-1} \theta_{12}^+}{g(\Theta)} \\ . & \frac{1}{1/g(\Theta)} \end{bmatrix}. \quad (3)$$

can be computed in  $\mathcal{O}(p^2)$  and satisfies  $[\mathbf{W}^+]^{-1} = \Theta^+$ .

*Proof.* By using the Banachiewicz inversion formula on Schur's complement (Zhang, 2006, Theorem 1.2)

$$\begin{bmatrix} \mathbf{W}_{11} & \mathbf{w}_{12} \\ \mathbf{w}_{21} & w_{22} \end{bmatrix} = \begin{bmatrix} \Theta_{11} & \theta_{12} \\ \theta_{21} & \theta_{22} \end{bmatrix}^{-1} = \begin{bmatrix} [\Theta_{11}]^{-1} + \frac{[\Theta_{11}]^{-1} \theta_{12} \theta_{21} [\Theta_{11}]^{-1}}{\theta_{22} - \theta_{21} [\Theta_{11}]^{-1} \theta_{12}} & -\frac{[\Theta_{11}]^{-1} \theta_{12}}{\theta_{22} - \theta_{21} [\Theta_{11}]^{-1} \theta_{12}} \\ . & \frac{1}{\theta_{22} - \theta_{21} [\Theta_{11}]^{-1} \theta_{12}} \end{bmatrix}. \quad (4)$$

Identifying all blocks yields  $[\Theta_{11}]^{-1} = \mathbf{W}_{11} - \frac{1}{w_{22}} \mathbf{w}_{12} \mathbf{w}_{12}^\top$  which can be computed in  $\mathcal{O}(p^2)$  if one has access to  $\mathbf{W}$ . This can be achieved using Equation (3), and involves only operations in  $\mathcal{O}(p^2)$ . The property  $\Theta^+ = [\mathbf{W}^+]^{-1}$  is satisfied by using the same inversion formula.  $\square$

Based on this result a full update of  $\Theta$  can be achieved with cost  $\mathcal{O}(p^3)$  ( $p$  column-row updates of cost  $\mathcal{O}(p^2)$ ).

## 4 Learning sparse precision matrices with SpodNet

In this section, we propose three specific SpodNet-based architectures for learning sparse precision matrices, which naturally arise in the context of Gaussian graphical models (Lauritzen, 1996) that we now briefly recall.

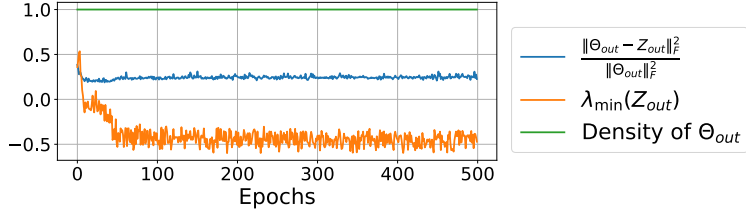


Figure 2: GLAD limitations: Smallest eigenvalue (orange), density degree (green) and relative discrepancy of the two matrices (blue) for one of the output  $(Z_{out}, \Theta_{out})$  of GLAD.  $\Theta_{out}$  and  $Z_{out}$  are significantly different,  $\Theta_{out}$  is not sparse, and  $Z_{out}$  is not positive-definite.

#### 4.1 A model-based formulation: the Graphical Lasso

Consider a dataset of  $n$  observed signals  $\mathbf{x}_1, \dots, \mathbf{x}_n$  where each  $\mathbf{x}_i \in \mathbb{R}^p$  follows a certain (centered) distribution with covariance matrix  $\Sigma \in \mathbb{S}_{++}^p$ . The problem of precision matrix estimation arises when attempting to identify the conditional dependency graph of the  $p$  variables of this dataset. Estimating these dependencies is of interest in many fields such as neuroscience (Rubinov and Sporns, 2010), finance (Ledoit and Wolf, 2003) or genomics (Cai et al., 2013). In Gaussian graphical models, this graph is associated with the so-called precision matrix  $\Theta = \Sigma^{-1}$  which directly encodes the dependencies<sup>1</sup>. The problem of precision matrix estimation involves determining  $\Theta \in \mathbb{S}_{++}^p$  given the empirical covariance matrix  $S = \frac{1}{n} \sum_{i=1}^n \mathbf{x}_i \mathbf{x}_i^\top$ . Moreover, in many practical situations the graph (thus the matrix  $\Theta$ ) is also sparse due to limited conditional dependencies, which leads to a sparse precision matrix estimation problem.

In this case, a very popular estimator is the Graphical Lasso (GLasso) (Banerjee et al., 2008; Friedman et al., 2008) that solves the convex optimization problem

$$\min_{\Theta \succ 0} -\log \det(\Theta) + \langle S, \Theta \rangle + \lambda \|\Theta\|_{1,\text{off}}, \quad (5)$$

where  $\|\Theta\|_{1,\text{off}}$  denote the off-diagonal  $\ell_1$  norm of  $\Theta$ , equal to  $\sum_{i \neq j} |\Theta_{ij}|$ . Equation (5) corresponds to an  $\ell_1$ -penalized maximum likelihood estimator under the assumption that the signals are Gaussian with covariance  $\Sigma$ . It can be computed with various convex optimization solvers, e.g. primal formulations (Mazumder and Hastie, 2012), proximal gradient descent (Rolfs et al., 2012), or second order algorithms (Hsieh et al., 2014), all with strict guarantees of recovering both sparse and SPD precision matrices. In particular, the algorithm of Mazumder and Hastie (2012) precisely fits the form of the updates in (2), where the functions  $f$  and  $g$  are not learnt, but correspond to solutions of changing Lasso regression problems.

Learning-based approaches, however, are scarcer. To the best of our knowledge, DeepGraph (Belilovsky et al., 2017) and GLAD (Shrivastava et al., 2019) are the only two existing works to tackle sparse precision matrix estimation under a data-driven perspective, both with restrictive limitations. This somewhat surprising fact is justified by the challenges posed by the task, which we highlight in the sequel.

#### 4.2 Limitations of learning-based approaches for sparse precision matrix estimation

**DeepGraph.** Belilovsky et al. (2017) propose to directly map empirical covariance matrices to the graph structures using a CNN-based architecture trained with supervision. DeepGraph is trained *for structure recovery only* and not for the estimation of the actual precision matrix. It disregards the magnitude of the elements of the output matrix and focuses solely on its support, thus circumventing the problem of SPD learning, which is a limitation for some applications.

**GLAD.** Shrivastava et al. (2019) unroll an alternating minimization algorithm for the Graphical Lasso (Dalal and Rajaratnam, 2017) to serve as an inductive bias for their model, which learns to predict elementwise regularization parameters of the updates. GLAD is trained with supervision, by minimizing a reconstruction error between the outputs and the ground truth matrix. The unrolled

<sup>1</sup>In this case  $\Theta_{ij} = 0$  iff variable  $i$  and  $j$  are conditionally independent, given the other variables.

algorithm is designed to solve a Lagrangian relaxation of (5)

$$\min_{\Theta, Z \in \mathbb{S}_{++}^p} -\log \det(\Theta) + \langle S, \Theta \rangle + \lambda \|Z\|_1 + \frac{\alpha}{2} \|Z - \Theta\|_F^2. \quad (6)$$

As detailed in [Appendix A.1](#), GLAD jointly operates on two matrices  $Z$  and  $\Theta$ . GLAD is a powerful model, and has a minimalist yet effective parametrization. Unfortunately, by treating  $Z$  and  $\Theta$  separately, the architecture cannot learn matrices that are *both sparse and SPD*. This is illustrated in [Figure 2](#) where  $\Theta$  and  $Z$  differ,  $\Theta$  is not sparse and  $Z$  is not SPD.

### 4.3 New models: SpodNet for learning sparse precision matrices

In this section, we present how to leverage SpodNet layers to overcome the limitations of existing solutions for learning both sparse and SPD precision matrices. By order of complexity, we present three neural architectures relying on SpodNet layers, each corresponding to a specific choice of the functions  $f$  and  $g$  in [Equation \(2\)](#).

All three architectures are inspired by an unrolling of a proximal block coordinate descent applied to the Graphical Lasso problem (5), where the blocks are column-row pairs described in [Section 3](#). Because (full) proximal gradient descent on (5) is called Graphical ISTA ([Rolfs et al., 2012](#)), we coin this Block-Graphical ISTA.

To derive its iterations, we note that the gradient of  $\Theta \mapsto -\log \det(\Theta) + \langle S, \Theta \rangle$  (the smooth term in the GLasso loss) is  $-\Theta^{-1} + S$  ([Boyd and Vandenberghe, 2004](#), Section A.4.1) and thus the gradient restricted to the  $\theta_{12}$ -block is  $-\Theta^{-1}_{12} + s_{12} = -w_{12} + s_{12}$ . Consequently, the proximal gradient descent algorithm on these coordinates writes  $\theta_{12}^+ = \text{prox}_{\lambda \gamma \|\cdot\|_1}(\theta_{12} - \gamma(s_{12} - w_{12}))$  where  $\gamma > 0$  is some stepsize and prox the proximal operator.

Using that the soft-thresholding is the proximal operator of the  $\ell_1$  norm, Block-Graphical ISTA hence reads

$$\theta_{12}^+ = \text{ST}_{\gamma \lambda}(\theta_{12} - \gamma(s_{12} - w_{12})). \quad (7)$$

**Unrolled Block Graphical-ISTA (UBG)** First, we propose to learn the stepsizes and soft-thresholding levels when unrolling the Block Graphical ISTA iterations (7). In a learning-based approach, we use as updating function  $f$ ,

$$f_{\text{UBG}} : \theta_{12} \mapsto \text{ST}_{\Lambda^+}(\theta_{12} - \gamma^+(s_{12} - w_{12})), \quad (8)$$

where the elementwise soft-thresholding parameters  $\Lambda^+$  along with the step-size  $\gamma^+$  are predicted by perceptrons at each update. We emphasize that this is different from hyperparameter tuning, since  $\gamma^+$  and  $\Lambda^+$  are predicted at each update instead of being global parameters. UBG exhibits the highest inductive bias among the models, as it's architecture is directly derived from unrolling an iterative optimization algorithm designed to minimize a model-based loss. Consequently, this architecture is particularly suited for learning sparse precision matrices.

However, as highlighted in [Section 3](#), the true power of SpodNet lies in the fact that one can plug *any* update functions and still get SPD outputs. This first motivates extending UBG to a more expressive setting with less inductive bias.

**Plug-and-Play Block Graphical-ISTA (PNP)** Next, we extend UBG to the Plug-and-Play setting ([Venkatakrishnan et al., 2013](#); [Romano et al., 2017](#); [Kamilov et al., 2023](#)). In a nutshell, these type of methods replace the proximal operator in first-order algorithms by a denoiser, usually implemented by a neural network. In our context, this corresponds to replacing the soft-thresholding of UBG by an arbitrary network  $\Psi : \mathbb{R}^{p-1} \rightarrow \mathbb{R}^{p-1}$ , that is,

$$f_{\text{PNP}} : \theta_{12} \mapsto \Psi(\theta_{12} - \gamma^+(s_{12} - w_{12})). \quad (9)$$

To promote sparsity of the output of  $f_{\text{PNP}}$ , the last layer of  $\Psi$  performs an elementwise soft-thresholding. The parameter for this soft-thresholding is also learned from the data and given by the same perceptron that predicts  $\Lambda^+$  in UBG.



Figure 3: Potential instabilities with no normalization: Along column update indices, we plot the smallest eigenvalue (blue), largest diagonal value (orange) and conditioning (green) of  $\Theta$ . We observe that  $\Theta$  remains SPD but gets increasingly closer to being singular during the updates.

**End-to-end Learnable Block Graphical-ISTA (E2E)** Finally, we propose a fully-flexible architecture without any algorithm-inspired assumptions. Precisely, we consider

$$f_{\text{E2E}} : \theta_{12}^+ \mapsto \Phi(\theta_{12}), \quad (10)$$

where  $\Phi$  takes in the current state of the column  $\theta_{12}$  and learns to predict an adequate column update  $\theta_{12}^+$ . Intuitively, the neural network  $\Phi$  acts as learning both the forward and the backward steps of a forward-backward iteration (Combettes and Pesquet, 2011). E2E is the most expressive of our three models because it is free from any inductive bias. As for PNP, sparsity of the predictions is enforced by a soft-thresholding non-linearity in the last layer of  $\Phi$ .

**Stability and update of the diagonal coefficient  $\theta_{22}$**  Although the positive definiteness of  $\Theta$  is guaranteed to be preserved at each update for any positive-valued function  $g$ , we have empirically observed that its smallest eigenvalue could approach 0 as visible in Figure 3. In practice this leads to instability in training. Below, we offer an interpretation of this phenomenon and suggest a solution to address it. Each column-row update inside a SpodNet layer can be written as the rank-2 update

$$\Theta^+ = \underbrace{\begin{bmatrix} \Theta_{11} & \theta_{12} \\ \theta_{21} & \theta_{22} \end{bmatrix}}_{=\Theta} + \underbrace{\begin{bmatrix} 0 & \theta_{12}^+ - \theta_{12} \\ (\theta_{12}^+ - \theta_{12})^\top & \theta_{22}^+ - \theta_{22} \end{bmatrix}}_{\triangleq \Delta_\Theta}. \quad (11)$$

Moreover, the nonzero eigenvalues of the perturbation  $\Delta_\Theta$  are given by  $\lambda_\pm = \frac{(\theta_{22}^+ - \theta_{22}) \pm \sqrt{(\theta_{22}^+ - \theta_{22})^2 + 4\|\theta_{12}^+ - \theta_{12}\|^2}}{2}$ , and by the Bauer-Fike theorem, we can quantify the evolution of  $\Theta$ 's spectrum by

$$|\lambda_k(\Theta) - \lambda_k(\Theta^+)| \leq \|\Delta_\Theta\|_{\text{op}}, \quad (12)$$

where  $\lambda_k$  denotes the  $k$ -th largest eigenvalue of a SPD matrix. Hence, one way to ensure that the perturbation of the spectrum is small is to control  $\|\Delta_\Theta\|_{\text{op}}$ , for instance, by limiting the magnitude of the updates. Experimentally, the most successful approach to control  $\|\Delta_\Theta\|_{\text{op}}$  is to limit the magnitude of  $\theta_{22}^+$ , which is not a trivial task as the updated value  $\theta_{22}^+ = g(\Theta) + \theta_{21}^+[\Theta_{11}]^{-1}\theta_{12}^+$  must satisfy  $\theta_{22}^+ - \theta_{21}^+[\Theta_{11}]^{-1}\theta_{12}^+ > 0$ . Thus, in practice we propose to scale  $\theta_{12}^+$ , ultimately choosing for all 3 models  $f \in \{f_{\text{UBG}}, f_{\text{PnP}}, f_{\text{E2E}}\}$  the column update

$$\theta_{12}^+ = \sqrt{\zeta} \frac{f(\Theta)}{\sqrt{f(\Theta)^\top [\Theta_{11}]^{-1} f(\Theta)}}, \quad (13)$$

which ensures that the diagonal update is given by  $\theta_{22}^+ = g(\Theta) + \zeta$ . The hyperparameter  $\zeta > 0$  acts as a form of regularization that handles a compromise between stability and expressivity of the model. In all of our experiments we set  $\zeta = 1$ .

Finally, for all models, we use for  $g$  a small neural network that takes as input the previous value of  $\theta_{22}$  and the corresponding diagonal entry of  $S$ ,  $s_{22}$ , and whose positivity is ensured by using an exponential function as final nonlinearity.

## 5 Experiments

We now illustrate our three graph learning models built on SpodNet layers's ability to learn relevant sparse precision matrices. This section aims to achieve two objectives. First, we highlight that

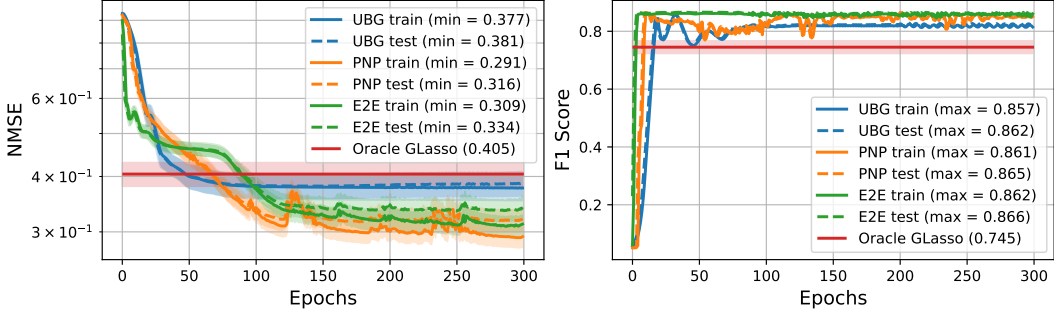


Figure 4: Training dynamics of our UBG, PNP and E2E models, compared to the baseline Oracle GLasso (in red) which provides both sparse and SPD matrices.

our three models learn matrices that are indeed sparse and SPD in contrast to other learning-based approaches such as GLAD. Second, we show that our models identify accurate sparse precision matrices and even outperform an oracle Graphical Lasso estimator.

**Data** We use synthetically generated data to fit our models. We generate  $N$  sparse SPD matrices of dimension  $p = 50$  using sklearn’s `make_sparse_spd_matrix` function (Pedregosa et al., 2011), of which we ensure proper conditioning by adding 0.1 to the diagonal entries. These matrices are treated as ground truth precision matrices  $\Theta_{\text{true}}^{(i)}$  for  $i \in [N]$ . The sparsity degree of each matrix is controlled through the one imposed on their Cholesky factors during their generation. We consider two setups for these sparse SPD matrices: weakly sparse ones ( $\alpha = 0.7$ ), and strongly sparse ones ( $\alpha = 0.95$ ). From each of these  $N$  ground truth precision matrices  $\Theta_{\text{true}} = \Sigma_{\text{true}}^{-1}$ , we sample  $n = 50$  i.i.d. centered Gaussian random vectors  $x_j \sim \mathcal{N}(0, \Sigma_{\text{true}}^{(i)})$ ,  $j \in [n]$ , which are used to compute an empirical covariance matrix  $S^{(i)}$ . Both the training and testing datasets thus comprise distinct couples  $(S^{(i)}, \Theta_{\text{true}}^{(i)})$ , meaning that each  $S^{(i)}$  stems from a different distribution. Since  $n = p$ , the  $S^{(i)}$ ’s are poorly conditioned and the estimation of  $\Theta_{\text{true}}^{(i)}$  is typically considered to be a very difficult problem to solve. We generate  $N_{\text{test}} = 100$   $(\Theta, S)$  couples for the testing set on which we evaluate all approaches. The average sparsity degrees of the ground truth in the weakly sparse and strongly sparse testing sets are respectively about 24% and 90%. The training set for our UBG model comprises 100 couples, whereas PNP and E2E are trained on 1000 couples.

**Minimization objective & performance metric** All three models are trained using ADAM with default parameters (Kingma and Ba, 2014) to minimize a reconstruction error loss  $\mathcal{L}_{\text{MSE}} = \frac{1}{N_{\text{train}}} \sum_{i=1}^{N_{\text{train}}} \|\hat{\Theta}^{(i)} - \Theta_{\text{true}}^{(i)}\|_F^2$  in the vein of GLAD, where  $N_{\text{train}}$  is the size of the training set and  $\hat{\Theta}$  is the model’s output.

**Architectures & training** We consider in our experiments models with  $K = 1$  SpodNet layer. The input to the models are the empirical covariance matrices  $S$ , from which we compute  $\Theta_{\text{init}} = (S + 0.1 * I)^{-1}$  and  $W_{\text{init}} = S + 0.1 * I$ , which serve as the inputs to the SpodNet layer. We use learning rates of 0.01, 0.02 and 0.03 respectively, to train UBG, PNP and E2E. The principal difficulty in training UBG and PNP stems from learning to predict  $\gamma^+$ . We find that using a perceptron with a single hidden layer of 10 neurons and ReLU activations that takes in the current state of the whole matrix to predict a  $\gamma^+$  is expressive enough to learn adequate matrices (Figures 4 and 6). Its positivity is ensured by taking the absolute value of the prediction. We believe that a more extensive architectural search for this perceptron could help achieve even better results. The prediction of the  $\Lambda^+$  parameters at each step is performed by a small single layer perceptron of 5 neurons with ReLU activation functions and an absolute value function following the last layer to ensure positivity. This network acts elementwise on the entries of the input vector. The sufficiency of a lower amount of training data for UBG could be imputed to its stronger inductive bias. PNP’s  $\Psi$  function and E2E’s  $\Phi$  function are learned by a single layer ReLU perceptron of 500 neurons. All experiments were ran on an RTX 2080 SUPER GPU with an AMD EPYC 7302 CPU and resources of similar computing power.

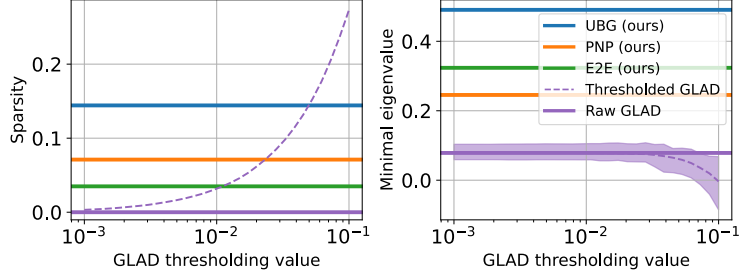


Figure 5: Sparsity (left) and positive-definiteness (right) of the raw predictions of all three of our models and GLAD’s, along with the latter’s thresholded predictions, on the testing set of the weakly sparse setting.

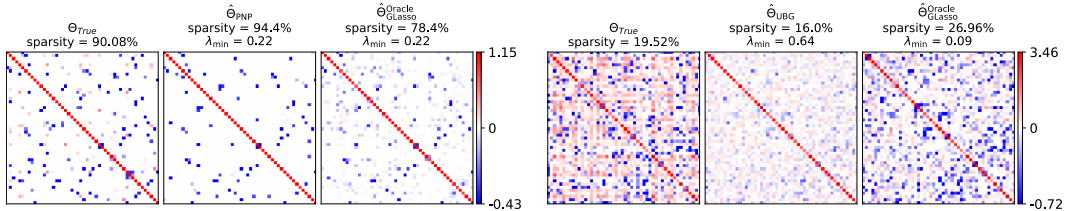


Figure 6: Comparison of sparsity degrees and smallest eigenvalues of UBG and PNP’s predictions with an Oracle GLasso, in both the strongly sparse (left panel) and weakly sparse (right) settings.

**Sparsity & positive-definiteness** Figure 5 highlights that all three of our models are indeed able to learn jointly sparse and SPD matrices. Contrary to GLAD, the raw predictions respect these structural constraints by construction. For the sake of completeness, we threshold the entries of GLAD’s raw predictions at increasing values to artificially introduce sparsity, and observe that this can indeed break their positive-definiteness. As visual confirmation, Figure 6 shows one of UBG and PNP’s predictions in the weakly sparse and strongly sparse settings.

**Performance & benchmark** Since GLAD’s predictions are not naturally sparse and SPD, we benchmark against sklearn’s implementation of the GLasso solver (Friedman et al., 2008), which is the standard algorithm for learning sparse precision matrices. We compare ourselves to an ideal *Oracle GLasso* where the  $\ell_1$  hyperparameter  $\lambda^{(i)}$  is individually assigned to the solver for each target matrix  $\Theta_{\text{true}}^{(i)} \forall i \in [N_{\text{test}}]$  and where  $\lambda^{(i)}$  is optimally tuned so as to achieve best possible reconstruction error. In practice, we validate this  $\lambda^{(i)}$  in  $[10^{-3} \lambda_{\max}, \lambda_{\max}]$  where  $\lambda_{\max}$  is the parameter such that every off-diagonal entry of the prediction is zero (see Appendix A.2). We emphasize that this is an idealistic scenario where the GLasso is at its most favorable. The results are depicted in Figure 4 for the weakly sparse setting and illustrates that our three models are indeed able to learn jointly sparse and SPD matrices while outperforming the Oracle GLasso solver. PNP yields the best performance in terms of NMSE whereas the E2E model is best in terms of support recovery in our setting. Figure 6 offers visual confirmation of the relevancy of the predictions. Interestingly, merely only one SpodNet layer is enough to achieve good performances for all of the three models.

## 6 Conclusion & future directions

We have proposed *Schur’s Positive-Definite Network* (SpodNet), a novel learning module compatible with other standard architectures offering strict guarantees of SPD outputs. The principal novelty of SpodNet comes from its higher expressivity than existing approaches, as it is also able to handle additional desirable structural constraints. In this work, we highlighted that it can be used to efficiently learn sparse and SPD matrices. To the best of our knowledge, SpodNet layers are the first to offer strict guarantees of such highly non-trivial structure in the outputs. We have shown how to leverage these guarantees to build several neural architectures that outperform the standard solvers in the context of sparse precision matrix estimation. Current directions of research include algorithmic

improvements in order to speed up SpodNet’s column/row/diagonal update framework and theoretical investigations in order to better understand the spectral perturbations undergone by the inputs.

## 7 Acknowledgments

We would like to thank Badr Moufad (Ecole Polytechnique, France) for his help with the PyTorch implementations of SpodNet, Paulo Gonçalves (Inria Lyon, France) for fruitful discussions as well as the Centre Blaise Pascal for computing ressources, which uses the SIDUS solution developed by Emmanuel Quemener (ENS Lyon, France) ([Quemener and Corvellec, 2013](#)). This work was partially supported by the AllegroAssai ANR-19-CHIA-0009 project.

## References

C. Bonet, B. Malézieux, A. Rakotomamonjy, L. Drumetz, T. Moreau, M. Kowalski, and N. Courty. Sliced-wasserstein on symmetric positive definite matrices for m/eeg signals. In *ICML*. PMLR, 2023.

C. Ju and C. Guan. Deep optimal transport for domain adaptation on spd manifolds. *arXiv preprint arXiv:2201.05745*, 2022.

O. Yair, F. Dietrich, R. Talmon, and I. G. Kevrekidis. Domain adaptation with optimal transport on the manifold of spd matrices. *arXiv preprint arXiv:1906.00616*, 2019.

S. L. Lauritzen. *Graphical models*. Clarendon Press, 1996.

X. S. Nguyen, L. Brun, O. Lézoray, and S. Bougleux. A neural network based on spd manifold learning for skeleton-based hand gesture recognition. In *CVPR*, 2019.

O. Ledoit and M. Wolf. Improved estimation of the covariance matrix of stock returns with an application to portfolio selection. *Journal of empirical finance*, 2003.

O. Ledoit and M. Wolf. A well-conditioned estimator for large-dimensional covariance matrices. *Journal of multivariate analysis*, 2004.

O. Banerjee, L. El-Ghaoui, and A. d'Aspremont. Model selection through sparse maximum likelihood estimation for multivariate gaussian or binary data. *JMLR*, 2008.

T. Cai, W. Liu, and X. Luo. A constrained  $\ell_1$  minimization approach to sparse precision matrix estimation. *Journal of the American Statistical Association*, 2011.

Z. Gao, Y. Wu, Y. Jia, and M. Harandi. Learning to optimize on spd manifolds. In *Proceedings of the IEEE/CVF Conference on Computer Vision and Pattern Recognition*, 2020.

K. Gregor and Y. LeCun. Learning fast approximations of sparse coding. In *ICML*, 2010.

Y. Chen and T. Pock. Trainable nonlinear reaction diffusion: A flexible framework for fast and effective image restoration. *IEEE transactions on pattern analysis and machine intelligence*, 2016.

V. Monga, Y. Li, and Y. C. Eldar. Algorithm unrolling: Interpretable, efficient deep learning for signal and image processing. *IEEE Signal Processing Magazine*, 2021.

T. Chen, X. Chen, W. Chen, H. Heaton, J. Liu, Z. Wang, and W. Yin. Learning to optimize: A primer and a benchmark. *JMLR*, 2022.

N. Boumal. *An introduction to optimization on smooth manifolds*. Cambridge University Press, 2023.

B. Rolfs, B. Rajaratnam, D. Guillot, I. Wong, and A. Maleki. Iterative thresholding algorithm for sparse inverse covariance estimation. *NeurIPS*, 2012.

D. Guillot and B. Rajaratnam. Functions preserving positive definiteness for sparse matrices. *Transactions of the American Mathematical Society*, 2015.

R. Sivalingam. *Sparse models for positive definite matrices*. PhD thesis, University of Minnesota, 2015.

R. Mazumder and T. Hastie. The graphical lasso: New insights and alternatives. *Electronic journal of statistics*, 2012.

P-A. Absil, R. Mahony, and R. Sepulchre. *Optimization algorithms on matrix manifolds*. Princeton University Press, 2008.

Z. Huang and L. Van Gool. A Riemannian network for SPD matrix learning. In *Proceedings of the AAAI conference on artificial intelligence*, 2017.

Z. Gao, Y. Wu, X. Fan, M. Harandi, and Y. Jia. Learning to optimize on riemannian manifolds. *IEEE Transactions on Pattern Analysis and Machine Intelligence*, 2022.

P-A. Absil and S. Hosseini. A collection of nonsmooth riemannian optimization problems. *Nonsmooth optimization and its applications*, 2019.

W. Huang and K. Wei. Riemannian proximal gradient methods. *Mathematical Programming*, 2022.

Y. Zhou, C. Bao, C. Ding, and J. Zhu. A semismooth newton based augmented lagrangian method for nonsmooth optimization on matrix manifolds. *Mathematical Programming*, 2023.

Z. Dong, S. Jia, C. Zhang, M. Pei, and Y. Wu. Deep manifold learning of symmetric positive definite matrices with application to face recognition. In *Proceedings of the AAAI Conference on Artificial Intelligence*, 2017.

D. Guillot and B. Rajaratnam. Retaining positive definiteness in thresholded matrices. *Linear algebra and its applications*, 2012.

H. Shrivastava. On using inductive biases for designing deep learning architectures. 2020.

H. Shrivastava, X. Chen, B. Chen, G. Lan, S. Aluru, H. Liu, and L. Song. Glad: Learning sparse graph recovery. In *ICLR*, 2019.

F. Zhang. *The Schur complement and its applications*, volume 4. Springer Science & Business Media, 2006.

M. Rubinov and O. Sporns. Complex network measures of brain connectivity: uses and interpretations. *Neuroimage*, 2010.

T. Cai, H. Li, W. Liu, and J. Xie. Covariate-adjusted precision matrix estimation with an application in genetical genomics. *Biometrika*, 2013.

J. Friedman, T. Hastie, and R. Tibshirani. Sparse inverse covariance estimation with the graphical lasso. *Biostatistics*, 2008.

C-J. Hsieh, M. A. Sustik, I. S. Dhillon, P. Ravikumar, et al. Quic: quadratic approximation for sparse inverse covariance estimation. *JMLR*, 15, 2014.

E. Belilovsky, K. Kastner, G. Varoquaux, and M. Blaschko. Learning to discover sparse graphical models. In *ICML*. PMLR, 2017.

O. Dalal and B. Rajaratnam. Sparse gaussian graphical model estimation via alternating minimization. *Biometrika*, 2017.

S. P. Boyd and L. Vandenberghe. *Convex optimization*. Cambridge university press, 2004.

S. V. Venkatakrishnan, C. A. Bouman, and B. Wohlberg. Plug-and-play priors for model based reconstruction. In *2013 IEEE global conference on signal and information processing*. IEEE, 2013.

Y. Romano, M. Elad, and P. Milanfar. The little engine that could: Regularization by denoising (red). *SIAM Journal on Imaging Sciences*, 2017.

Ulugbek S Kamilov, Charles A Bouman, Gregory T Buzzard, and Brendt Wohlberg. Plug-and-play methods for integrating physical and learned models in computational imaging: Theory, algorithms, and applications. *IEEE Signal Processing Magazine*, 40(1):85–97, 2023.

P. L. Combettes and J-C. Pesquet. Proximal splitting methods in signal processing. *Fixed-point algorithms for inverse problems in science and engineering*, 2011.

F. Pedregosa, G. Varoquaux, A. Gramfort, V. Michel, B. Thirion, O. Grisel, M. Blondel, P. Prettenhofer, R. Weiss, V. Dubourg, J. Vanderplas, A. Passos, D. Cournapeau, M. Brucher, M. Perrot, and E. Duchesnay. Scikit-learn: Machine learning in Python. *Journal of Machine Learning Research*, 12:2825–2830, 2011.

D. P. Kingma and J. Ba. Adam: A method for stochastic optimization. *arXiv preprint arXiv:1412.6980*, 2014.

E. Quemener and M. Corvellec. Sidus—the solution for extreme deduplication of an operating system. *Linux Journal*, 2013, 2013.

## A Supplementary Material

### A.1 GLAD's update rules

Each unrolled iteration of GLAD, which can be seen as an individual layer in a deep learning perspective, updates several running variables:

$$\alpha^+ = \tilde{f}(\|\mathbf{Z} - \Theta\|_F^2, \alpha), \quad (14)$$

$$\mathbf{Y}^+ = \frac{1}{\alpha^+} \mathbf{S} - \mathbf{Z}, \quad (15)$$

$$\Theta^+ = \frac{1}{2} \left( -\mathbf{Y}^+ + \sqrt{\mathbf{Y}^{+\top} \mathbf{Y}^+ + \frac{4}{\alpha^+} \mathbf{Id}} \right), \quad (16)$$

$$\lambda_{ij}^+ = \tilde{h}(\Theta_{ij}^+, S_{ij}, Z_{ij}), \quad (17)$$

$$Z_{ij}^+ = \text{ST}_{\lambda_{ij}^+}(\Theta_{ij}^+), \quad \forall i, j \in [p], \quad (18)$$

in which the functions  $\tilde{f} : \mathbb{R}^2 \rightarrow \mathbb{R}$  and  $\tilde{h} : \mathbb{R}^3 \rightarrow \mathbb{R}$  are two small neural networks that are trained to predict adequate parameters for each layer. By construction,  $\Theta^+$  is always SPD and a sparsity structure is enforced on  $\mathbf{Z}^+$ , but the converse is not true.

### A.2 Critical regularization parameter for the Graphical Lasso

**Proposition A.1.** *Let  $\hat{\Theta} = \operatorname{argmin}_{\Theta} -\log \det \Theta + \langle \mathbf{S}, \Theta \rangle + \lambda \|\Theta\|_{1,\text{off}}$ . Then,  $\hat{\Theta}$  is diagonal if and only if  $\lambda \geq \lambda_{\max} = \max_{i \neq j} |s_{ij}|$ .*

*Proof.* The first-order optimality condition, aka Fermat's rule, for the Graphical Lasso is:

$$\hat{\Theta} = \operatorname{argmin}_{\Theta} -\log \det \Theta + \langle \mathbf{S}, \Theta \rangle + \lambda \|\Theta\|_{1,\text{off}} \Leftrightarrow \hat{\Theta}^{-1} + \mathbf{S} \in \partial \|\hat{\Theta}\|_{1,\text{off}} \quad (19)$$

Now  $\mathbf{U} \in \partial \|\hat{\Theta}\|_{1,\text{off}}$  if and only if

- $U_{ii} = 0$  for  $i \in [p]$
- $U_{ij} \in \lambda \partial |\Theta_{ij}| = \begin{cases} \lambda \operatorname{sign}(\Theta_{ij}) & \text{if } \Theta_{ij} \neq 0 \\ [-\lambda, \lambda] & \text{otherwise} \end{cases} \quad \text{for } i, j \in [p], i \neq j.$

Hence

$$\hat{\Theta} \text{ is diagonal} \Leftrightarrow \hat{\Theta}^{-1} \text{ is diagonal} \quad (20)$$

$$\Leftrightarrow s_{ij} \in [-\lambda, \lambda] \quad \forall i \neq j \quad (21)$$

$$\Leftrightarrow \lambda \geq \lambda_{\max} = \max_{i \neq j} |s_{ij}| \quad (22)$$

□